PRIFYSGOL

BANGOR

UNIVERSITY

1884

Drought-related mortality modifies mixing effects on light absorption and growth in mono-specific and mixed stands of Fagus sylvatica, Alnus glutinosa and Betula pendula.

Plaga, Benjamin; Bauhus, Jürgen; Smith, Andy; Gonzalez Pereira, Mario ; Forrester, David

Forestry

Cyswllt i'r cyhoeddiad / Link to publication

16. Nov. 2023

Drought-related mortality modifies mixing effects on light absorption and growth in mono-specific and mixed stands of *Fagus sylvatica*, *Alnus glutinosa*, and *Betula pendula*

Benjamin N.E. Plaga[1], Jürgen Bauhus[1], Andrew R. Smith[2], Mário G. Pereira[3] and David I. Forrester[4],*

[1]Institute of Forest Sciences, Faculty of Environment and Natural Resources, University of Freiburg, Tennenbacherstrasse 4, 79106 Freiburg, Germany
[2]Environment Centre Wales, School of Natural Sciences, Bangor University, Bangor, Gwynedd LL57 2DG, United Kingdom
[3]Centre for Research and Technology of Agro-Environmental and Biological Sciences (CITAB), Inov4Agro, University of Trás-os-Montes and Alto Douro (UTAD), Quinta de Prados, 5000-801 Vila Real, Portugal
[4]CSIRO Environment, GPO Box 1700, Canberra, ACT 2601, Australia
*Corresponding author. CSIRO Environment, GPO Box 1700, Canberra, ACT 2601, Australia. E-mail: David.Forrester@csiro.au

Abstract

Little is known about how drought-related mortality influences light absorption of surviving trees and consequent changes in tree species interactions. Here, we used the detailed tree-level light model (Maestra) in combination with measurements of tree dimensions, crown architectures, and stand structures to examine experimental mixing effects of *Fagus sylvatica*, *Alnus glutinosa*, and *Betula pendula* on light dynamics following a drought in Bangor, Wales. The experimental stands, planted in 2004, were composed of clusters with one to three species in different combinations. Droughts occurred in 2011 and 2014 during the growing seasons, and trees were measured in 2014 and 2015. Species mixing resulted, on average, in higher tree growth, absorption of photosynthetically active radiation (APAR), and light-use efficiency (LUE) compared with the mean of the monocultures. An exception was the monoculture of *B. pendula*, which was the most productive species and had higher growth, APAR, or LUE than some mixtures. Drought-related mortality reduced the stand basal area across all plots by an average of 8.3% and tree density by 11%. This moderate change in the structure did not result in significant increases in individual tree APAR, LUE, or growth. From a management perspective, mortality might need to reduce stand density more strongly than it did in this study before light absorption or LUE is altered.

Keywords: light absorption; light-use efficiency; mixed-species forests; Maestra model; drought-related mortality; tree allometry

Introduction

The increasing frequency, duration, and intensity of droughts is impacting different types of forest ecosystems in many regions of the world (IPCC 2013). Tree mortality rates are increasing in many forest types and climate zones as a consequence of drought, water stress, and the subsequently increased activity of biotic agents (Allen et al. 2010, 2015). This mortality can strongly modify stand structure and thus ecosystem functioning (Klos et al. 2009, Lindner et al. 2010, Anderegg et al. 2013, Bennett et al. 2015, Clark et al. 2016, Seidl et al. 2017). To assess potential options to increase the resilience and adaptive capacity of forests in relation to climate change, it is important to know how mortality-driven changes in structure influence ecosystem functions and services. Processes such as light absorption, light-use efficiency, and subsequent growth of remaining trees will likely play a central role in the ecosystem response to tree mortality.

Currently, establishing mixed-species forests is seen as one of the main strategies to increase resistance, resilience, and adaptive capacity in relation to climatic change (Bauhus et al. 2017a, Messier et al. 2022); in addition, mixed-species forests can be more productive than the mean of the individual species monocultures (Zhang et al. 2012, Jactel et al. 2017, Feng et al. 2022). One of the causes of the higher productivity of mixtures is light-related species interactions (Binkley et al. 1992, Forrester et al. 2012, 2018, Sapijanskas et al. 2014). Absorption of photosynthetically active radiation (APAR) and light-use efficiency (LUE) in mixtures are influenced by canopy stratification (Binkley et al. 1992, Forrester et al. 2012, le Maire et al. 2013), different crown shapes and architectures (Bauhus et al. 2004, Sapijanskas et al. 2014, Forrester et al. 2018), inter-specific differences in physiology and phenology (Binkley et al. 1992, Augspurger and Bartlett 2003, Lopez et al. 2008, Forrester et al. 2012, Vitasse 2013, Sapijanskas et al. 2014, Gressler et al. 2015), and stand density (Will et al. 2005, Forrester et al. 2013, 2018, Sapijanskas et al. 2014, Dong et al. 2016).

Increases in canopy tree mortality rates may alter the interactions between species within mixtures. Mortality leads to open spaces in forest canopies, similar to thinning from above, and can also change the vertical structure by removing species or trees that occupy specific positions within the canopy, e.g. a thinning from below that removes overtopped and intermediate trees or

subcanopy species. Thinning usually leads to an increase in the productivity of the residual trees (Smith et al. 1997, Bauhus et al. 2017b), which may partly be caused by an increase in APAR or LUE of retained individual trees. West and Osler (1995) found an increase in individual tree growth after thinning on two sites of *Eucalyptus regnans*, which resulted from higher individual tree APAR. When there was no understory, thinning also resulted in higher individual tree LUE. Increases in individual tree APAR and LUE following thinning have also been reported in other studies (Forrester et al. 2013, Gspaltl et al. 2013). Tree loss by mortality, although a more gradual process than tree removal through thinning, could have similar effects to thinning on APAR, LUE, and growth.

Unlike thinning, the effect of natural mortality on APAR and LUE in mixed-species forests has received very little attention. Therefore, the objective of this study was to examine how mortality in a tree diversity experiment influenced tree and stand APAR and LUE. The experiment contained plots with one-, two-, and three-species mixtures of *Fagus sylvatica*, *Alnus glutinosa*, and *Betula pendula* in Bangor, Wales. All plots that were examined for this study included drought-induced tree mortality and were measured in the year that followed the drought.

We tested the following hypotheses:

(1) Increases in APAR and LUE are both responsible for complementary effects on tree growth in mixtures compared with monocultures.
(2) Intra-specific differences in crown architecture (in addition to inter-specific differences) contribute to increases in APAR and LUE in mixtures.
(3) A reduction in stand density due to mortality results in an increase in individual tree growth, APAR, and LUE.

Materials and Methods
Site description and experimental design

The investigations took place in some of the plots within the BangorDIVERSE experiment which is part of TreeDivNet, a global network of tree diversity experiments. It was established with a total area of 2.36 ha in March 2004 at the Henfaes Research Centre of Bangor University in Wales (UK) (53° 14′ 16.382″ N, 4° 1′ 0.922″ W) at 13–18 m a.s.l. near the coast (Ahmed et al. 2016). Soils are classified as Eutric Fluvic Cambisols (IUSS Working Group WRB 2006) (Fluventic Dystrochrept, USDA system) and have fine loamy texture (Smith et al. 2013).

The experiment has a hexagonal planting design where each species was planted with an inter-tree spacing of 1×1 m^2 (10 000 trees ha^{-1}). Each hexagonal plot originally contained 94 trees and a two-row buffer strip with an additional 78 trees. In the plots that were examined in this study, the species pool containing *A. glutinosa*, *B. pendula*, and *F. sylvatica* was used to create a diversity gradient comprising one-, two-, and three-species communities. This study was performed in all species combinations (*n* = 7) that occurred in oval or circular clusters of trees (Fig. 1), and each of the hexagonal plots was replicated five times, totaling 35 clusters. The two-row buffer strip combined with the gradual change in species composition within each hexagon, from one cluster to the next, is expected to minimize any potential edge effects between species combinations. During data collection late in the summer of 2015, it was noticed that a considerable proportion of trees had died since the inventory in 2014. Using the meteorological data that were logged on-site, we identified droughts occurring in 2011 and 2014, especially during the growing seasons when only half of the

long-term average precipitation occurred (Table 1). Prior to 2011, there had been negligible mortality within the plots.

Quantification of the vertical structure and distribution of leaf area and leaf area density

All tree diameters at 1.3 m (diameter growth at breast height; DBH) were measured in April 2014 and September 2015. To quantify the leaf area and leaf area density distribution of each tree, we took detailed tree measurements for each of the three species on one individual in each species combination (cluster) and replicated it in each plot in 2015. This procedure included measuring the following variables: diameter at 1.30 m, height, live-crown length, crown area, as well as the diameters, heights, and cardinal directions (divided into eight segments: N, NE, E, SE, S, SW, W, NW) of all branches on each of the sample trees. In addition, the mean branch angle from the horizontal was estimated for each quarter of the live-crown length. A sample branch was then taken from each quarter of these target trees to measure the mean leaf angles from the horizontal, the branch length, leaf area, and leaf dry mass. For the latter, all leaves were removed from the sample branches, dried at 70°C, and weighed. Before drying, the leaf area of a subsample was determined using a leaf area meter LI-3050C Transparent Belt Conveyor Accessory (LI-COR Biosciences GmbH, Bad Homburg, Germany) to calculate the specific leaf area (m^2 kg^{-1}) for the branch and thus the leaf area from the product of specific leaf area and leaf dry weight of the branch.

In the next step, we used the branch measurements to develop allometric equations (as shown in Equation 1) for each species to calculate all branch lengths within the crowns and the leaf area of all target trees:

$$\ln(Y) = \ln \beta_0 + \beta_1 \ln \left(d_b \right) + \beta_2 \ \ln(rh) + \beta_3 \left(\ln \left(d_b \right) * \ln(rh) \right) + \varepsilon \quad (1)$$

Where Y is the branch length or branch leaf area, d_b is the branch diameter, *rh* is the relative height of the branch within the live-crown length (base = 1, top = 0), and ε is a correction ratio used when back-transforming the ln-transformed Y-variables. The correction ratio was calculated as the sum of the measured values divided by the sum of the (back-transformed) predicted values (Snowdon 1991). The leaf area of a given branch was assumed to be distributed evenly between the base of the branch, where it joined the tree stem, and the height of the branch tips, which was calculated using the branch length and branch angle measurements as described in Medhurst and Beadle (2001) and Forrester et al. (2013). In the last step, the leaf area density (LAD, m^2 m^{-3}) was calculated by dividing the total crown into 10 layers. Each layer contributed 10% of the live-crown length and was assumed to have a volume of a semi-elliptical cone for the top layer or a frustum of a semi-elliptical cone for the other nine layers (Equation 2). The vertical distribution of LAD was fitted to a beta distribution (Equation 3, Wang et al. 1990) where the LAD of a layer was a function of its relative height within the crown. The parameters of this equation are required inputs to run the Maestra model (Grace et al. 1987, Wang and Jarvis 1990, Medlyn 2004, Duursma and Medlyn 2012), which was used to calculate individual tree APAR:

$$V = \frac{2}{3}\pi * h * r2 + \sum_{l=2}^{10} h * \left(d_{basal}2 + d_{top}2 + d_{basal} * d_{top} \right) * \frac{\pi}{12} \quad (2)$$
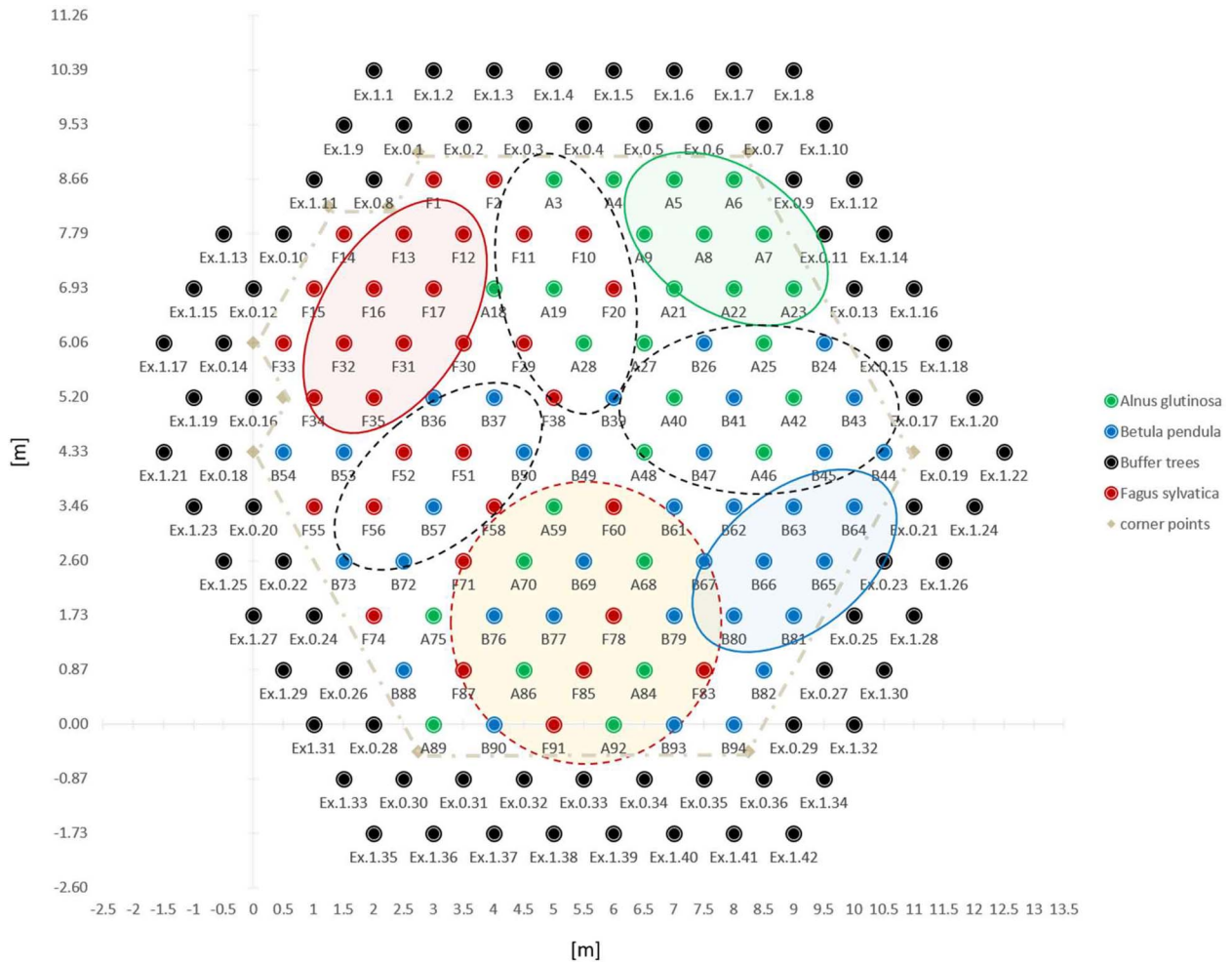
Figure 1. Planting design of the mixing experiment hexagonal plots, which was replicated five times; A_x with green dot = *A. glutinosa*; B_x with blue dot = *B. pendula*; F_x with red dot = *F. sylvatica*; $Ex_{x.x}$ with black dots = buffer trees. The ovals with solid borderlines indicate mono-specific clusters, the ovals with dashed lines indicate clusters with two-species mixtures, and circles with dashed lines comprise tree clusters with the three-species mixture. The design minimizes edge effects by placing similar cluster next to each other. Edge effects were not addressed in the analysis.

Table 1. Mean annual precipitation, temperature, and aridity index at the experiment.

	All year			Growing season (DOY = 111–303)		
	1979–2017	2011	2014	1979–2017	2011	2014
Precipitation (mm)	1013.1	471.8	621.2	567.4	270.8	270.4
Mean temperature (°C)	9.4	11.4	11.9	12.65	14.0	14.5
Aridity Index	52.2	22.1	28.4	25.1	11.5	11.1

DOY are the Julian days 111 and 303 of the year that define the growing season. The aridity index is calculated from the amount of precipitation (*P*) and temperature (*T*) as $P/(T + 10)$ (Martonne 1926).

where *V* is the total crown volume, *h* is the height of the layer, *r* is the radius of the cone for the top layer, d_{basal} is the crown diameter of the base of the frustrum, and d_{top} is the crown diameter of the top.

$$Y = a\left(x^b\right) * (1 - x)^{cc} \tag{3}$$

Where *a*, *b*, and *cc* are fitted parameters, and *Y* is the leaf area density ($m^2\,m^{-3}$) at a relative height of *x* within the canopy.

Field measurements and quantification of structure and growth at the tree and stand levels

In addition to the target trees mentioned above for which we measured individual tree leaf area (*la*), crown diameter, and

vertical distribution of LAD, we also measured height and live-crown length for all trees within the plot, as well as DBH of all trees within the plot and the surrounding buffer trees. For all other trees, including buffer trees, the height, leaf area, crown diameter, and live-crown length were determined by predicting these variables as a function of DBH, separately for each species (Equation 4):

$$\ln(Y) = \ln \beta_0 + \beta_1 \ln(DBH) + \varepsilon \tag{4}$$

Where *Y* is height, leaf area, crown diameter, and live-crown length, and ε is a correction ratio used when back-transforming the ln-transformed *Y*-variables. The correction ratio was calculated as the sum of the measured values divided by the sum of

the (back-transformed) predicted values (Snowdon 1991). Individual crown volumes (m³) were calculated for each tree from their crown diameter and live-crown length by assuming semi-elliptical shapes (Equation 2).

Individual tree basal area increment (cm² year⁻¹) was calculated by combining the DBH measurements from 2015 with those of the previous inventory in 2014. We also recorded trees that had recently died due to drought. This allowed us to use our allometric equations to calculate all variables for trees that were alive in the previous inventory. We were therefore able to quantify the structure of the plots before and after the drought-related tree death. The Maestra model was then used to calculate the individual tree APAR for two cases: (i) following the mortality event (all trees that have died have no leaves) and (ii) for the same structure as if no trees had died during the drought, assuming all trees still have leaves.

Stand variables calculated included the relative height, mean stand height (m), tree density (trees ha⁻¹), leaf area index (m² m⁻²), basal area (m² ha⁻¹), basal area increment (m² ha⁻¹ year⁻¹), canopy depth (m), canopy volume(m³ ha⁻¹), and canopy–leaf area density (m² m⁻³). The relative height of a given species was calculated as the mean height of the target species divided by the mean height of the total cluster. The canopy depth was calculated from the difference between the height of the tallest tree in a cluster and the height of the crown base of the tree with the lowest crown in that cluster.

To illustrate the change in stand structure caused by drought-related mortality, we examined diameter distributions corrected for the species proportions (Supplementary Figs S1–S3; Fig. 3). That is, the number of trees in each diameter class was divided by the proportion of stand basal area contributed by that species (not by the diameter class). The trend curves (Fig. 3) were obtained using Friedman's SuperSmoother (Friedman 1984b, 1984a) to smooth the (*x,y*) values. We used the R function "supsmu," from the "stats" package and R 4.0.3 (R Core Team 2020), which is a running lines smoother that chooses between three spans for the lines (Friedman 1984b, 1984a). The running lines smoothers are symmetric, with *k*/2 data points on each side of the predicted point, and values of *k* as 0.5 × *n*, 0.2 × *n*, and 0.05 × *n*, where *n* is the number of data points. The best of the three smoothers was chosen by cross-validation for each prediction. The best spans were then smoothed using the running lines smoother and the final prediction chosen by linear interpolation.

Climate data

We obtained meteorological data from the ERA-Interim reanalysis daily dataset produced by the European Centre for Medium-Range Weather Forecasts with a high spatial resolution (0.125° × 0.125°) (Dee et al. 2011). The climatic variables included monthly and daily mean temperature, precipitation, solar radiation, and the number of frost days. We extracted daily data on surface solar radiation downwards (SSRD), from 2012 to 2017 and monthly climate data from 1979 to 2017. In addition, we obtained on-site meteorological data (based on hourly means) from the Henfaes Research Centre of Bangor University for 2004–2014 to determine the precipitation pattern for this period. The solar radiation was used as input to the Maestra model to calculate APAR and LUE.

MAESTRA light modeling to estimate APAR

Individual tree APAR was calculated using the MAESTRA model (Grace et al. 1987, Wang and Jarvis 1990, Medlyn 2004, Duursma and Medlyn 2012). This 3D tree-level model calculates individual trees' APAR based on their individual crown architecture (e.g.

crown dimensions and leaf area and leaf angle distributions), leaf optical properties (leaf transmittance and reflectance), and the shading from neighboring trees based on the positions of other trees within the plot (defined by *x* and *y* coordinates, the slope and aspect of the site) and their crown architectures (e.g. Fig. 2).

The growing season was defined by the site-specific phenology of the leaf-bearing period of the three species we studied. This was from Julian day 111 to Julian day 303. APAR was calculated for the growing season (defined by the leaf-bearing period) and also for the whole year. The parameterization data we used are provided in Supplementary Table S1.

Estimation of LUE and relative productivity

Tree level LUE (cm² GJ⁻¹) was calculated as the basal area increment of the individual tree (cm² year⁻¹) per APAR (GJ year⁻¹). Stand-level LUE (m² GJ⁻¹) was calculated as the basal area increment of the whole community (cluster) (m² ha⁻¹ year⁻¹) per APAR (GJ ha⁻¹ year⁻¹).

The relative productivity (RP) variable (Equations 5 and 6) quantifies whether mixing led to an increase (RP > 1) or decrease (RP < 1) in a given variable compared with a monoculture at the stand level, per species (Equation 6), or the whole plot community (Equation 5) (Williams and McCarthy 2001, Forrester and Pretzsch 2015). The RP also accounts for the proportion of the species in the mixtures, which was quantified in terms of leaf area index (LAI; m² m⁻²) or stand basal area, depending on the response variable. For response variables tree density, basal area, and basal area increment, we quantified the species proportions in terms of stand basal area. All other proportions for the canopy and light variables (canopy depth, volume, proportion of canopy filled with tree crowns, LAD, APAR, and LUE) were quantified in terms of LAI because it is considered more representative of the species contributions to light dynamics, and species proportions by leaf area have been shown to provide realistic estimates of species proportions on an area basis (Dirnberger and Sterba 2014):

$$\text{RP}_{\text{community}} = \frac{p_{mix^{sp1,sp2,...}}}{\because_{sp1}p_{mono^{sp1}} + \because_{sp2}p_{mono^{sp2}} + \ldots} \quad (5)$$

$$\text{RP}_{\text{species}} = \frac{p_{mix^{sp1,(sp2...)}}}{\because_{sp1}p_{mono^{sp1}}} \quad (6)$$

In Equation (5), $p_{mix^{sp1,sp2}}$ is the productivity (or the performance of another response variable) of the mixed-species stand in relation to the productivity of their related monocultures ($p_{mono^{sp1}}$, $p_{mono^{sp2}}$) and their proportional ($\because_{sp1}$, $\because_{sp2}$) amount of LAI or stand basal area depending on the stand variable considered. Equation (6) is used to determine the relative productivity by species where $p_{mix^{sp1,(sp2)}}$ is the productivity of a given species (sp1) in a mixture with (sp2).

Statistical analysis

Differences between species mixing treatments or between species were examined using a Tukey test. All variables were visually assessed for normality. Regression models were fitted as hierarchical mixed-effects models using the R package nlme (Pinheiro et al. 2020) and R 4.0.3 (R Core Team 2020). To ensure that residuals were centered at zero and approximately normally distributed, the residual and normal quantile plots were assessed. For branch-level regressions, the random effect was tree nested within plot, and for tree-level regressions the random effect was the plot.
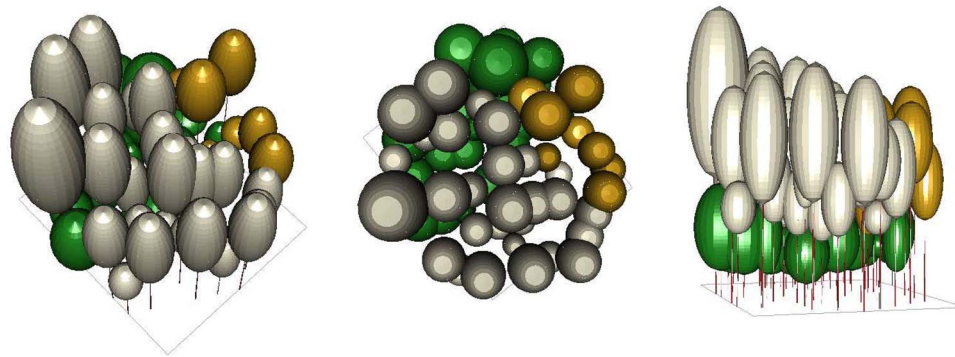
Figure 2. 3D representation of one plot with all seven clusters without the buffer tree rows illustrating the canopy structure in terms of vertical stratification, canopy gaps and closure, horizontal overlapping and interlocking of the crowns. Trees with green crowns represent *F. sylvatica*, gray represents *B. pendula*, and golden brown shows *A. glutinosa*.

Results

Tree-level effects of mixing, mortality, and stand structure

Across all clusters, the highest mortality rate occurred in *A. glutinosa*, which resulted in a 21% reduction in basal area and a 32% reduction in tree density (Supplementary Table S2). The greatest reduction in *A. glutinosa* density occurred in the three-species mixture and included trees from all diameter classes. In the monoculture and two-species mixtures, mortality decreased from smaller to medium diameter classes (Supplementary Fig. S2a–d).

For *A. glutinosa*, DBH, height, live-crown length, and crown volume were larger in the mixture with *B. pendula* than in monoculture (Table 2). When in combination with *F. sylvatica*, *B. pendula* crown parameters were not significantly larger, but DBH and leaf area were higher compared with monocultures (Table 2). We found these differences in terms of the mixture before as well as after tree mortality, but we found no effect within the mixtures and within the monoculture due to mortality. When *A. glutinosa* and *B. pendula* were mixed with the smaller *F. sylvatica*, the relative height increased accordingly for both species and decreased for *F. sylvatica*. APAR was higher for the trees in two-species mixtures without any *B. pendula* compared with the trees in monocultures or the three-species mixture. This mixing effect only occurred for stands containing *B. pendula* after the occurrence of mortality (Table 2), which was the largest in these clusters. Basal area growth and LUE increased when growing with *F. sylvatica* (Table 2).

Drought-related mortality decreased the basal area of *B. pendula* by 3.1% and tree density by 9.9% (Supplementary Table S2). Only the smallest diameter classes were affected and almost all of them were in the monoculture and the three-species mixture (Supplementary Fig. S3a–d). Nearly all examined tree variables, except LUE, increased for *B. pendula* when mixed with *F. sylvatica* (Table 2). In contrast, when *B. pendula* was combined with *A. glutinosa* or was in the three-species mixture, there were no significant changes in its tree-level variables when compared with the monoculture. There was no significant effect on these mixing results due to mortality within these clusters.

Unlike *B. pendula*, *F. sylvatica* showed a reduction in some variables in the two-species combination with *B. pendula* (Table 2). Since basal area growth remained the same, while a reduction in APAR occurred, this led to a higher LUE compared with monocultures (Table 2). The relative height of *F. sylvatica* was reduced by the presence of the two taller tree species in mixtures. Nevertheless, with *A. glutinosa* as a neighbor, *F. sylvatica* was able to increase live-crown length, leaf area, crown volume, and also APAR (Table 2).

In the three-species mixture, in addition to the higher live-crown length, crown volume, and APAR, *F. sylvatica* even achieved higher basal area growth as well as an increase in LUE (Table 2). Mortality in *F. sylvatica* was negligible.

We did not detect any major shifts in species proportions due to mortality (Fig. 3e–l). However, there were small shifts in tree size distributions toward larger diameter classes for *B. pendula* and *A. glutinosa*, while for *F. sylvatica*, the smallest species, the mortality of the other two species caused a corresponding shift toward the smaller diameter classes (Fig. 3e–l).

Individual tree APAR was positively correlated with tree leaf area for all species (Supplementary Fig. S4). For a given tree leaf area, APAR of *B. pendula* was significantly greater in three-species mixtures and when combined with *F. sylvatica*, but significantly lower when mixed with *A. glutinosa* than in monocultures. *Alnus glutinosa* in a mixture with *F. sylvatica* and in three-species mixture had a significantly greater APAR for a given leaf area compared with their monoculture. For *F. sylvatica*, APAR remained the same as in all treatments (Supplementary Fig. S4).

Stand-level effects of mixing and mortality

Mortality within clusters reduced basal area by 8.3% and density by 11% (Supplementary Table S2). As the smaller and medium diameter classes within the two larger species were mainly affected by mortality, there was a decrease in the frequency of these diameters for the total stands of the two- and three-species mixtures (Fig. 3a–d). The visual inspection of the diameter class distribution was only changed by mortality in the three-species mixture, where we observed a shift toward the smaller diameter classes (Fig. 3d).

The two-species mixture of *F. sylvatica* and *B. pendula* showed higher tree density, LAI, canopy depth, canopy volume, and a higher proportion of filled canopy space when compared with the monoculture of *B. pendula* (Supplementary Table S3, Fig. 4a and c). Compared with the *F. sylvatica* monoculture, canopy depth and canopy volume as well as basal area and basal area growth were also higher in the mixture (Supplementary Table S3; Fig. 4a and d). Both species absorbed more PAR in two-species mixture than the respective monocultures (Fig. 4e; Supplementary Table S3). The mixture of these species also achieved the highest overall values in terms of canopy volume, LAI, basal area increment, and APAR compared with all other clusters (Fig. 4a, c–e).

The combination of *B. pendula* and *A. glutinosa* led to higher total means of LAI, canopy depth, canopy volume, basal area, and basal area increment as well as higher APAR when compared with the

Table 2. Mean tree variables in a planted tree diversity experiment for each species across all monocultures and mixtures in Bangor.

Variable	Monoculture		2-species mixture		2-species mixture		3-species mixture		P value		
F. sylvatica (*n* = 145 | *n* = 146)			+ *A. glutinosa*		+ *B. pendula*		+ *A. glutinosa* + *B. pendula*		Div.level	Mortality	Interaction
Diameter (cm)	2.35^a	2.38^a	**2.75**^{a}	**2.75**^{a}	1.93^b	1.93^b	2.56^a	2.56^a	<0.0001	0.921	0.998
Height (m)	**4.17**^{a}	**4.21**^{a}	4.59^a	4.59^a	3.58^b	3.58^b	4.25^a	4.25^a	<0.0001	0.927	0.999
Crown diameter (m)	4.23^{bc}	4.26^{ab}	4.57^a	4.57^a	3.93^c	3.93^c	4.37^{ab}	4.37^{ab}	<0.0001	0.941	1
Live-crown length (m)	**2.89**^{a}	**2.91**^{a}	3.70^b	3.70^b	2.61^a	2.61^a	3.49^b	3.49^b	<0.0001	0.956	1
Height to the live crown (m)	**1.28**^{a}	**1.3**^{a}	0.89^{bc}	0.89^{bc}	0.97^b	0.97^b	0.76^c	0.76^c	<0.0001	0.926	0.999
Leaf area (m^2)**	4.80^a	4.94^a	6.87^b	6.87^b	3.33^c	3.33^c	5.81^{ab}	5.81^{ab}	<0.0001	0.922	0.999
Crown volume (m^3)**	**29.12**^{ac}	**29.67**^{a}	43.87^b	43.87^b	22.33^c	22.33^c	36.93^b	36.93^b	<0.0001	0.946	1
Relative height	**1**^{a}	**1**^{a}	0.81^b	0.83^b	0.56^c	0.56^c	0.67^d	0.68^d	<0.0001	0.671	0.972
APAR (GJ tree^{-1} season^{-1})*	0.79^a	0.84^{ab}	1.21^{bc}	1.31^c	0.53^d	0.56^{ad}	1.16^{bc}	1.25^c	<0.0001	0.487	1
APAR (MJ per tree per day)*	2.16^a	2.29^{ab}	3.30^{bc}	3.59^c	1.45^d	1.54^{ad}	3.19^{bc}	3.42^c	<0.0001	0.487	1
Basal area growth (cm^2 year^{-1})*	**0.64**^{a}	**0.65**^{a}	0.74^{ab}	0.74^{ab}	0.63^a	0.63^a	0.82^b	0.82^b	<0.0001	0.946	1
Light-use efficiency (cm^2 GJ^{-1})*	**0.69**^{a}	**0.69**^{a}	0.73^{abd}	0.71^{ab}	0.84^{cd}	0.82^{bcd}	0.92^c	0.89^c	<0.0001	0.513	0.974
B. pendula (*n* = 132 | *n* = 145)			+ *A. glutinosa*		+ *F. sylvatica*		+ *A. glutinosa* + *F. sylvatica*		Div.level	Mortality	Interaction
Diameter (cm)	**5.46**^{a}	**5.89**^{a}	5.91^a	5.91^a	7.31^b	7.74^b	5.87^a	6.03^a	0.0003	0.427	0.960
Height (m)	7.83^b	8.25^{ab}	7.87^b	7.87^b	8.89^{ab}	9.23^b	8.09^b	8.25^{ab}	**0.019**	0.399	0.952
Crown diameter (m)*	**3.36**^{a}	**3.44**^{a}	3.54^{ac}	3.54^{ac}	3.91^{bc}	4.03^b	3.54^a	3.58^{ac}	**0.0006**	0.461	0.972
Live-crown length (m)	4.07^a	4.31^{ab}	4.48^{ab}	4.48^{ab}	5.15^{bc}	5.40^c	4.49^{ab}	4.59^{ab}	**0.0045**	0.488	0.976
Height to the live crown (m)	3.75^a	3.92^a	3.38^a	3.38^a	3.73^a	3.48^a	3.62^a	3.67^a	0.159	0.563	0.978
Leaf area (m^2)**	**4.58**^{a}	**5.14**^{a}	5.28^{ac}	5.28^{ac}	7.16^{bc}	7.85^b	5.23^a	5.48^{ac}	**0.0006**	0.421	0.960
Crown volume (m^3)*	**29.31**^{a}	**33.05**^{a}	34.75^{ab}	34.75^{ab}	49.31^{bc}	56.15^c	34.75^{ab}	36.53^{ab}	**0.002**	0.454	0.967
Relative height	**1**^{a}	**1**^{a}	0.98^a	0.97^a	1.4^{bc}	1.44^b	1.27^c	1.32^{bc}	<0.0001	0.493	0.937
APAR (GJ per tree per season)*	**1.95**^{a}	**2.47**^{a}	2.15^a	2.26^a	4.16^{bc}	4.98^b	2.5^a	2.93^{ac}	**0.0001**	0.181	0.965
APAR (MJ per tree per day)*	**5.34**^{a}	**6.72**^{a}	5.90^a	6.14^a	11.41^{bc}	13.66^b	6.79^a	8.04^{ac}	**0.0001**	0.181	0.965
Basal area growth (cm^2 year^{-1})*	2.53^a	2.77^{ab}	3.1^{abc}	3.1^{abc}	4.02^{bc}	4.57^c	2.72^a	2.92^{ab}	**0.009**	0.489	0.982
Light-use efficiency (cm^2 GJ^{-1})	0.90^a	0.83^a	0.97^a	0.93^a	0.84^a	0.92^a	0.74^a	0.73^a	0.219	0.883	0.943
A. glutinosa (*n* = 42 | *n* = 68)			+ *B. pendula*		+ *F. sylvatica*		+ *B. pendula* + *F. sylvatica*		Div.level	Mortality	Interaction
Diameter (cm)	**5.21**^{b}	**5.55**^{ab}	6.41^{ae}	6.86^{de}	7.72^{cd}	8.46^c	6.05^{abe}	6.80^{acde}	<0.0001	0.091	0.947
Height (m)	**6.94**^{b}	**7.23**^{ab}	8.31^{cd}	8.89^c	7.99^{acd}	8.19^{acd}	7.48^{abd}	8.23^{abcd}	0.0005	0.133	0.902
Crown diameter (m)	3.12^b	3.22^{ab}	3.28^{ab}	3.38^{ab}	3.54^a	3.69^a	3.31^{ab}	3.51^{ab}	0.066	0.322	0.993
Live-crown length (m)	**3.19**^{a}	3.18^a	**4.38**^{bc}	4.69^b	3.56^{ac}	3.60^{abc}	3.60^{ac}	3.72^{abc}	**0.001**	0.727	0.9770
Height to the live crown (m)	3.81^a	4.09^a	3.91^a	4.18^a	4.44^a	4.58^a	3.89^a	4.47^a	0.438	0.276	0.967
Leaf area (m^2)	2.97^b	3.16^{ab}	4^{abc}	4.37^{ac}	4.32^c	4.73^c	3.7^{abc}	4.26^{abc}	**0.002**	0.272	0.979
Crown volume (m^3)*	17.15^a	17.68^{ab}	27.44^{bc}	30.64^c	24.1^{abc}	25.33^{abc}	23.62^{abc}	26.9^{abc}	**0.009**	0.569	0.999
Relative height	**1**^{a}	**1**^{a}	1.06^{ac}	1.09^{ac}	1.36^b	1.43^b	1.9^{cd}	1.32^{bd}	<0.0001	0.179	0.689
APAR (GJ per tree per season)	1.15^a	1.41^{ab}	1.93^{bc}	2.40^c	2.42^c	2.76^c	1.89^{bc}	2.14^{abc}	<0.0001	0.134	0.986
APAR (MJ per tree per day)	3.15^a	3.87^{ab}	5.30^{bc}	6.57^c	6.61^c	7.55^c	5.17^{bc}	5.86^{abc}	<0.0001	0.134	0.986
Basal area growth (cm^2 year^{-1})*	1.17^{bc}	1.23^{abc}	1.48^{ab}	1.82^{ae}	2.32^{de}	3.0^d	0.92^c	1.05^{abc}	<0.0001	0.187	0.884
Light-use efficiency (cm^2 GJ^{-1})**	**0.58**^{a}	**0.58**^{a}	0.69^{ac}	0.95^{abc}	1.95^{bc}	2.67^b	0.15^a	0.24^a	0.0001	0.492	0.933

APAR was predicted using the MAESTRA model. Trees were planted in 2004 and measured in 2015. For a pair of columns for a given treatment, the left column shows means calculated assuming no drought-related mortality, while the right column shows the means following the mortality. Values printed in bold and with different letters within a row indicate significant differences between mixing treatments and mortality (*P* < 0.05). Compact letter display of all pairwise comparisons of least-squares means was generated using the R function "cld" implemented in the multcomp package (Piepho 2004). Significance of diversity treatments (Div.level), mortality, and their interaction are provided in the three right columns. *Values were ln-transformed before back transformed by Snowdon ratio (Snowdon 1991). **Values were sqrt-transformed before back transformed by Snowdon ratio (Snowdon 1991).

monoculture of *A. glutinosa* but not when compared with the *B. pendula* monoculture (Supplementary Table S3; Fig. 4a, c–e).

The two-species mixture of *F. sylvatica* and *A. glutinosa* resulted in higher tree density, LAI, canopy depth, canopy volume, proportion of filled canopy space, and APAR in comparison with the monoculture of *A. glutinosa,* and higher canopy depth and basal area, but lower proportion of filled canopy space, than in the *F. sylvatica* monoculture (Supplementary Table S3, Fig. 4a, c, e). Both basal area increment and LUE were also higher in the mixture than in respective monocultures. Here, after the onset of mortality, LUE for *A. glutinosa* became higher in the mixture than in the monoculture (Supplementary Table S3; Fig. 4f). No other mortality effects were significant.

The three-species mixture showed higher tree density, LAI, canopy depth, canopy volume, proportion of canopy space filled, and APAR when compared with *A. glutinosa* monocultures and lower tree density and proportion of canopy space filled, but higher basal area and canopy depth, when compared with *F. sylvatica* monocultures before and after the drought-related mortality, except APAR which was also higher in the three-species mixture before mortality than in *F. sylvatica* monocultures (Supplementary Table S3; Fig. 4b, c, e). There were no significant differences between response variables in *B. pendula* between its monoculture and the three-species mixture, except for *canopy depth*. This pattern did not change with the following mortality.
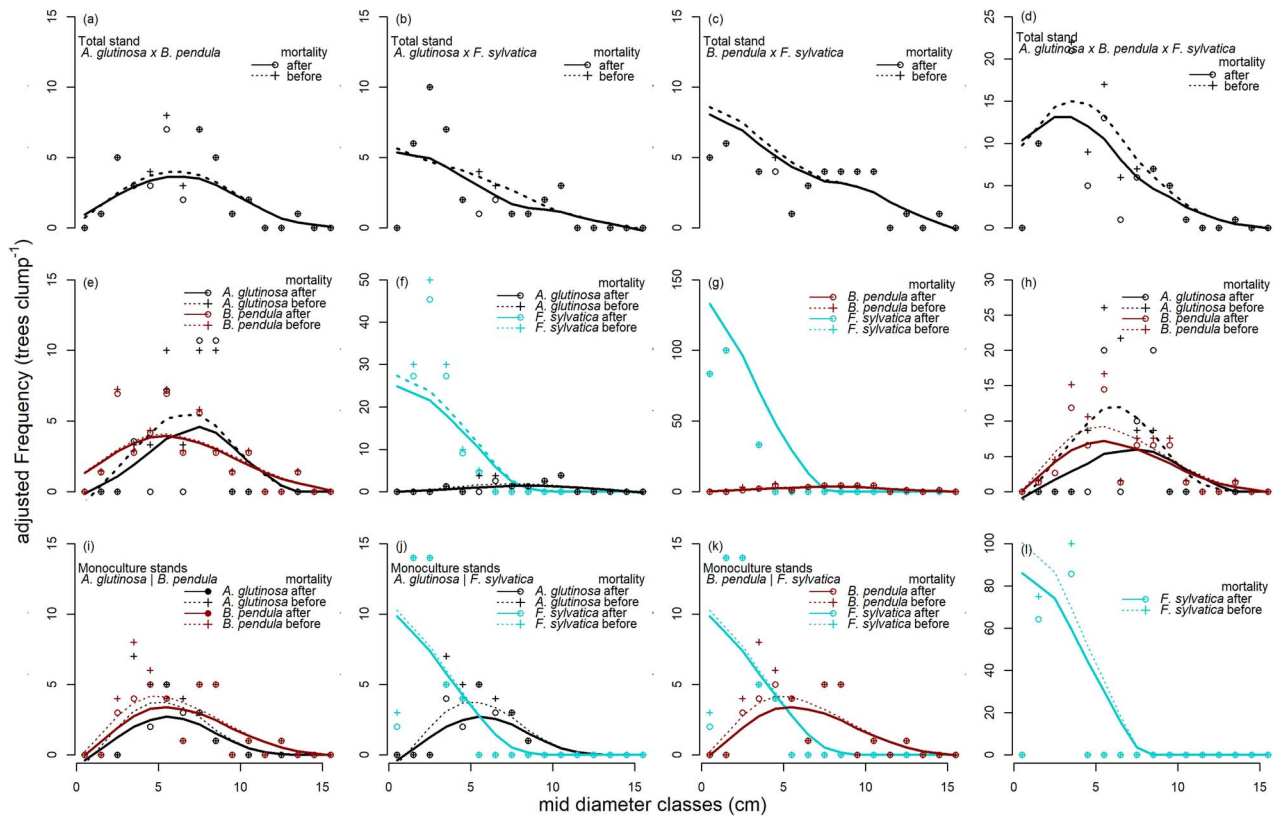
Figure 3. Size distributions illustrating the change in stand structure caused by drought-related mortality in *A. glutinosa–B. pendula* stands (**a**, **e**, **i**), *A. glutinosa–F. sylvatica* stands (**b**, **f**, **j**), *B. pendula–F. sylvatica* stands (**c**, **g**, **k**), and all three species (**d**, **h**, **l**). The size class is 1 cm. Trend curves were plotted by the use of Friedman's SuperSmoother (Friedman 1984a, 1984b) to smooth the (*x*, *y*) values. Note the different scales on the *y*-axes.

Diversity-level effects of mixing and mortality

On average, mortality reduced basal area across the three diversity levels by 16.2% across all three-species mixtures, 8.9% across all monocultures, and 5.2% in the two-species mixtures (Supplementary Table S2). In terms of diversity level, two-species mixtures benefited most compared with monocultures regarding nearly all variables (Supplementary Table S4, Fig. 5a, c–f). The three-species mixtures also benefited compared with monocultures, except for tree density, basal area, and LUE (Supplementary Table S4; Fig. 5a, c–e). The canopy leaf area density was highest in monocultures and significantly lower in the mixtures, which then did not differ further among the different mixtures. Within a diversity level, mortality only led to a significant reduction in tree density in the three-species mixture (Supplementary Table S4). As a result of this mortality, the APAR of three-species mixtures was significantly lower than in two-species mixtures, which was not the case before the mortality occurred (Fig. 5e). In contrast, mortality within the three-species mixtures resulted in a slightly non-significant increased LUE, which was then not statistically different from the two-species mixtures whereas this was the case before the mortality occurred (Supplementary Table S4; Fig. 5f).

Discussion

The basal area growth was lower, on average, in the monocultures (0.95 m^2 ha^{-1} year^{-1}) than in the two-species mixtures (2.1 m^2 ha^{-1} year^{-1}) and three-species mixture (1.4 m^2 ha^{-1} year^{-1}). This was associated with higher APAR in the two-species mixtures (18.3 GJ ha^{-1} 10^{-3}) and three-species mixture (15.2 GJ ha^{-1} 10^{-3}) when compared with the monocultures (11.3 GJ ha^{-1} 10^{-3}).

The stand LUE was also higher in the two-species mixtures (109 m^2 GJ^{-1} × 10^6) and three-species mixture (92 m^2 GJ^{-1} × 10^6) than in the monocultures (73 m^2 GJ^{-1} × 10^6). These findings are in accordance with hypothesis 1 and with results from other studies which showed that higher growth in mixtures is often associated with increases in both APAR and LUE (Binkley et al. 1992, Forrester et al. 2012, Forrester and Albrecht 2014, Forrester 2019). Here, this result is predominantly attributable to tree species identity effects. For example, *B. pendula* was generally more productive and had higher APAR and LUE than the other species and also maintained these advantages when growing in mixtures (Fig. 4d–f). Similarly, LAI was highest in *F. sylvatica* monocultures and when this species was present in the mixtures, it increased LAI and canopy volumes in these stands. As a result, the *F. sylvatica–B. pendula* mixture had the highest APAR of any treatment, regardless of mortality effects (Fig. 4a, c, e). Species identity appears to have been an important determinant of mixing effects on growth and APAR in most studies (e.g. le Maire et al. 2013, Forrester et al. 2019). This enhancement of APAR, and hence the growth of mixtures, was probably at least partly caused by inter-specific differences in tree size (crowns, heights, crown lengths), crown architecture (leaf angles), tree allometry, and the effect these had on canopy attributes (e.g. varying leaf area density, canopy stratification, canopy volume). Inter-specific differences in physiology, such as photosynthetic rates, LUE, and the often observed synergistic effect of mixing fast-growing shade-intolerant species with initially slow-growing shade-tolerant species, may also have contributed to mixing effects on LUE, as was found in previous studies (Binkley et al. 1992, Forrester et al. 2012, Baeten et al. 2019, Serrano-León et al. 2022).
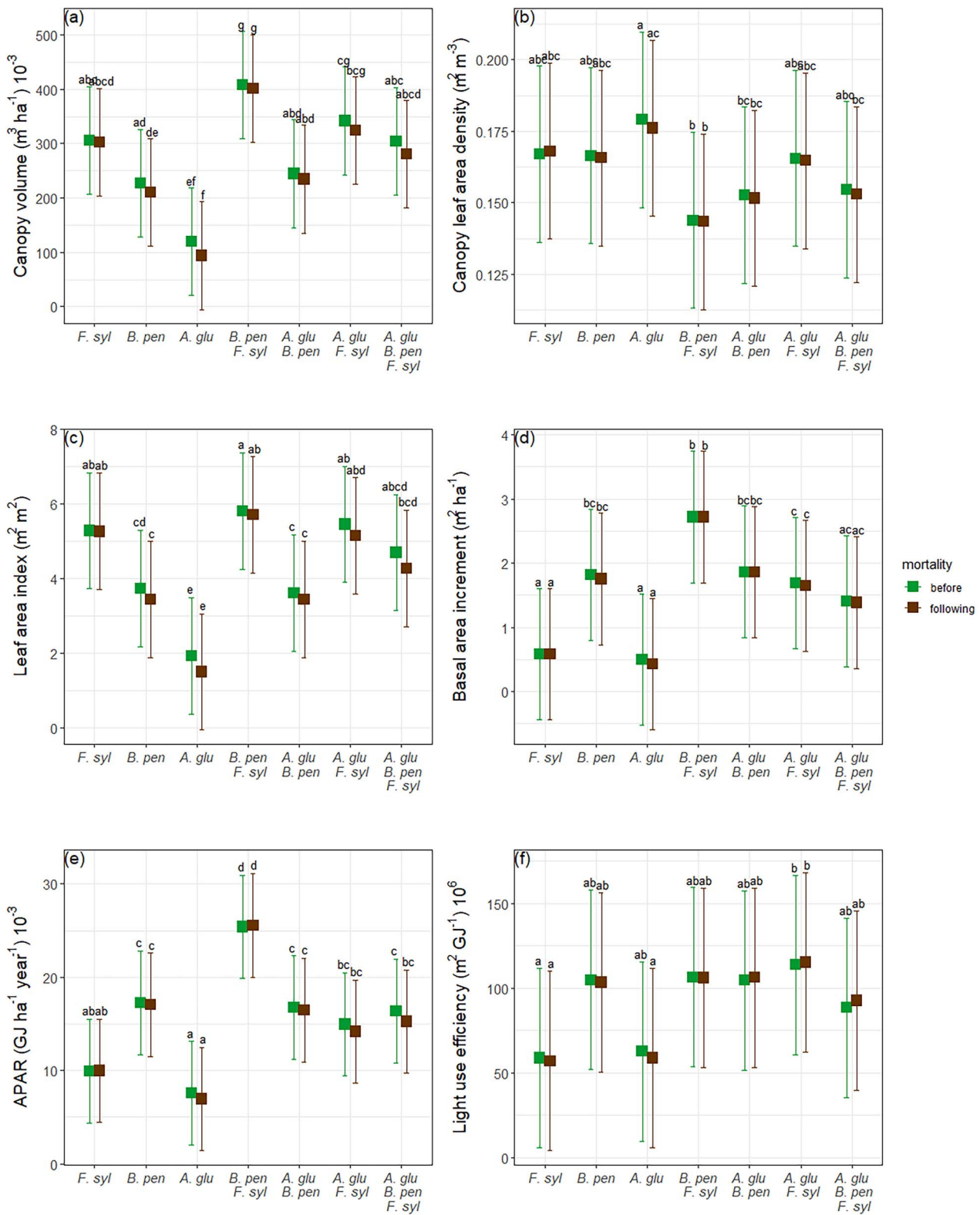
Figure 4. Means of canopy volume (**a**), canopy leaf area density (**b**), leaf area index (**c**), stand basal area increment (**d**), annual absorption of photosynthetic active radiation APAR (**e**), and light-use efficiency (**f**) with and without recently died trees across all monocultures and mixtures. *F. syl* = *F. sylvatica*, *B. pen* = *B. pendula*, *A. glu* = *Alnus glutinosa* in monoculture. *B. pen F. syl*, *A. glu F. syl*, and *A. glu F. syl* = species combination in two-species mixture. *A. glu, B. pen, F. syl* = three-species mixture. Error bars indicate the 95% confidence interval of LS mean. Means sharing a letter are not significantly different (Tukey-adjusted comparisons (*P* value) with significance level alpha = 0.05; variables and residuals were visually inspected for normality).
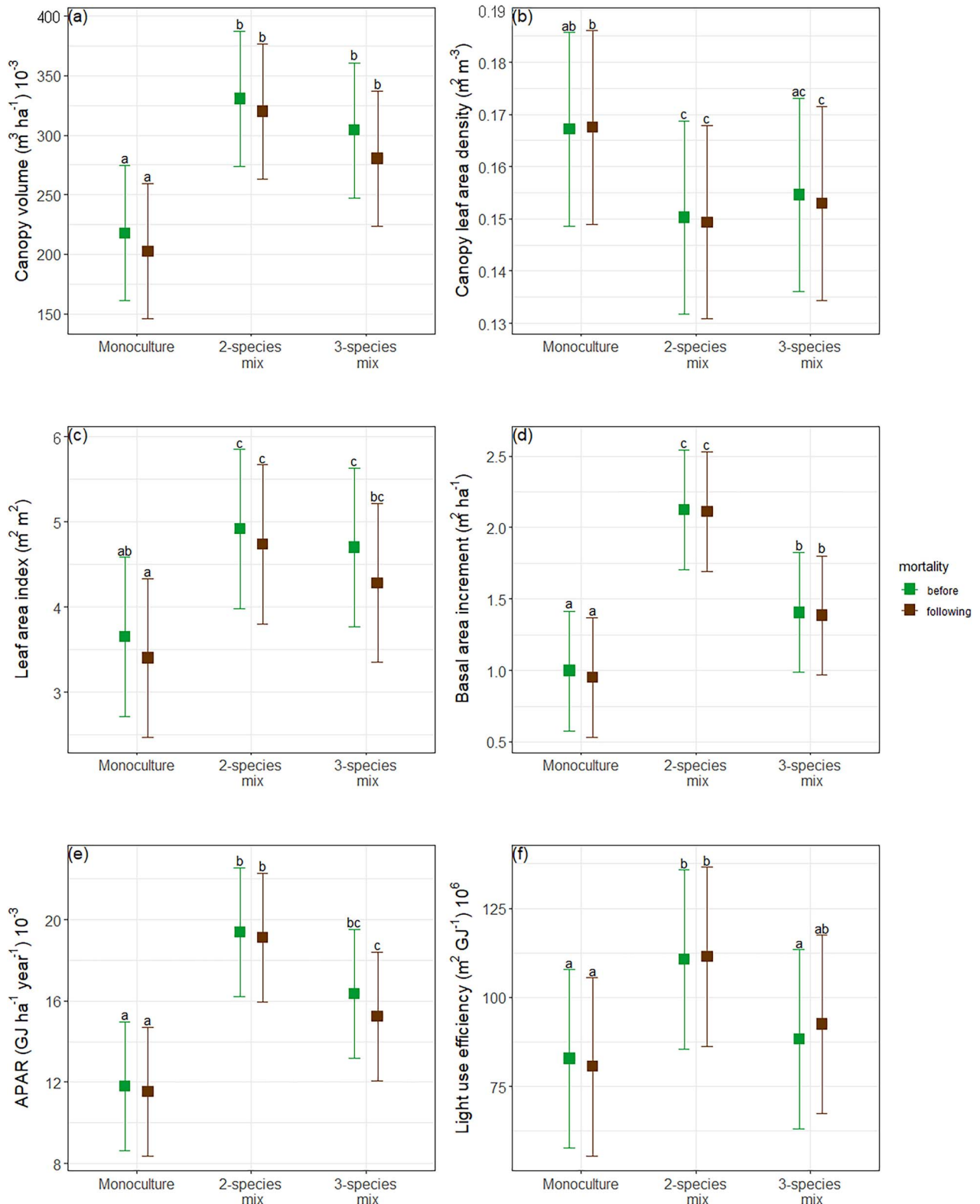
Figure 5. Means of canopy volume (**a**), canopy leaf area density (**b**), leaf area index (**c**), stand basal area increment (**d**), annual absorption of photosynthetic active radiation APAR (**e**), and light-use efficiency (**f**) with and without recently died trees across all three diversity levels. Error bars indicate the 95% confidence interval of LS mean. Means sharing a letter are not significantly different (Tukey-adjusted comparisons (P value) with significance level alpha = 0.05; variables and residuals were visually inspected for normality).

Differences in growth or light absorption have also been linked to intra-specific differences in physiology, mean tree sizes, crown architectures (e.g. leaf angles), and allometric relationships between stem size and crown characteristics (Sapijanskas et al. 2014, Dong et al. 2016, Forrester et al. 2018, Serrano-León et al. 2022). In this study, there were only minor differences in allometric relationships (e.g. Fig. S4) and specific leaf area for a given species in the different species combinations. Therefore, intra-specific variability may not have been as important in these stands. There were also negligible shifts in the partitioning of light between size classes, such that competition for light for all species was generally size-symmetric or slightly asymmetric as indicated by the linear relationships between individual tree leaf area and APAR (Fig. S4). While these findings contradict our second hypothesis that intra-specific differences in crown architecture (in addition to inter-specific differences) contribute to increases in APAR and LUE in these mixtures, similar results have been obtained in previous studies (e.g. Forrester 2019, Plaga et al. "in review").

The drought-related mortality reduced stand basal area by only 8.5% and tree density by 11%. This minor reduction in stand density had no significant influence on stand growth, APAR, or LUE and no influence on individual tree growth following the drought. This is consistent with many thinning studies showing that minor changes in stand density (<20% reduction in basal area) have little influence on growth (Stoneman et al. 1996, Mäkinen and Isomäki 2004, Will et al. 2005). Studies that found such effects on growth and APAR were typically conducted at much higher thinning intensities, for example, with a 65% reduction in tree density (Forrester 2013) or a 74% reduction in basal area (West and Osler 1995, Gspaltl et al. 2013). This indicates that unless mortality removes much larger proportions of stand density, it is unlikely to influence APAR.

Given the strong correlation between radiation, temperature, and vapor pressure deficit under forest canopies, the minimal effects of mortality on APAR in this study may be associated with minimal effects on below canopy microclimates. Therefore, mortality or thinning events that remove small proportions of overstorey stand basal area may have a negligible influence on the ability of forests to function as an insulator for understorey communities (Davis et al. 2018, von Arx et al. 2012, Zellweger et al. 2020).

A small effect of mortality could only be observed for *A. glutinosa*, where mortality reduced their basal area across all stands by 21% and even 63% in the three-species stands (Supplementary Table S2) in which all diameter classes of *A. glutinosa* were affected. This supports our assessment that APAR or LUE will only change significantly when larger proportions of the stand density die. The reason for the much higher drought-related mortality in *A. glutinosa* may be attributed to its preference for moist to wet soil conditions (Houston Durrant et al. 2016, CABI 2022). Although we observed a few small changes in growth, APAR, and LUE due to mortality, the gradient in mortality across the experiment was too small to robustly test the third hypothesis, that a reduction in stand density due to mortality results in an increase in individual tree growth, APAR, and LUE. Changes in the structure after drought could probably similarly influence APAR, but for this to happen, the effects of drought must be much stronger than in this study.

The results of this study should be interpreted with caution when extrapolating to other forests given the young age of this experiment (10 years old), the high planting density of 10 000 plants per hectare, and the strong influence that site conditions (e.g. resource availability and climatic conditions) can have on mixing effects. Crowns may be more responsive at this age than in older stands, and as trees age there are changes in crown architecture and morphology (e.g. specific leaf area, leaf angle distributions), and canopy structure that can influence APAR. Furthermore, drought can influence mortality for several years following the end of a drought and our data collected only 1 year after the drought may hence not yet capture all effects induced by the drought (Bigler et al. 2006, 2007, Cailleret et al. 2017, Klockow et al. 2018, Powers et al. 2020, Trugman et al. 2021). In our experiment, there was negligible mortality prior to 2011, and therefore, we assume that the majority of mortality in this study was caused by drought. Trees that appeared to be dying in 2015 did not recover, and we assumed there was negligible additional mortality after our measurements until another severe drought in 2018, so it is likely that the major influence of the 2011 and 2015 droughts on APAR was quantified. Given that all plots were influenced by the drought, it is not possible to distinguish the effect of changes in density on tree growth and LUE from those caused by water stress during the drought.

The magnitudes of the mixing effects found in this study should not be extrapolated to other sites, given that the relative sizes of mixing effects on growth can change with resource availability and climatic conditions (e.g. Forrester 2014). These spatial dynamics of mixing effects could be examined by replicating mixtures along site gradients in resource availability and climatic conditions. They could also be predicted using process-based models that have been validated for their ability to predict mixing effects in forests, such as the 3-PG model (e.g. Forrester et al. 2017a).

The estimates of APAR obtained using the Maestra model in this study will be influenced by the model inputs for each individual tree. It was not possible to measure the leaf areas, vertical crown leaf area density distributions, or leaf angles for all trees and therefore allometric relationships were used. Allometric relationships between tree size and foliage mass or area for a given species can change when it is growing in a mixture with other species (e.g. Laclau et al. 2008) and due to stand density (e.g. Monserud and Marshall 1999, Forrester et al. 2017b). Similarly, mixing can influence the vertical distribution of leaf area within tree crowns (Garber and Maguire 2005, Binkley 1992). Therefore, trees from all treatments were sampled and used to derive the inputs for the Maestra model. We assume that the APAR estimates used in this study are reliable because the mixing effects on allometry and vertical crown leaf area density distributions were accounted for, and several studies have found accurate comparisons between Maestra predictions of APAR and observed APAR or APAR estimated using hemispherical photography (Charbonnier et al. 2013, le Maire et al. 2013, Forrester et al. 2018, 2019).

Conclusion

In conclusion, species mixing increased growth, APAR, and LUE compared with the mean of the monocultures, with the exception of the most productive monoculture of *B. pendula*. The reduction in stand density caused by drought-related mortality was too small to notably influence APAR, LUE, or growth. This is consistent with previous studies where greater reductions in density by thinning were required to significantly increase APAR. With regards to forest management, minor reductions in stand density may be unlikely to cause significant effects on stand APAR, LUE, or growth.

Acknowledgements

CRediT statement

Benjamin Plaga (Data curation, Formal analysis, Investigation, Methodology, Writing—original draft, Writing—review and editing), Juergen Bauhus (Conceptualization, Project administration, Resources, Supervision, Writing—review and editing), Andy Smith (Conceptualization, Data curation, Resources, Writing—review and editing), Mário Gonzalez Pereira (Data curation, Resources, Writing—review and editing), and David Forrester (Conceptualization, Formal analysis, Investigation, Methodology, Project administration, Resources, Supervision, Writing—original draft, Writing—review and editing)

Supplementary Data

Supplementary data are available at *Forestry* online.

Conflict of interest

None declared.

Funding

Data availability

The data underlying this article will be shared on reasonable request to the corresponding author.

References

Ahmed IU, Smith AR, Jones DL. *et al.* Tree species identity influences the vertical distribution of labile and recalcitrant carbon in a temperate deciduous forest soil. *For Ecol Manage* 2016;**359**:352–60. https://doi.org/10.1016/j.foreco.2015.07.018.

Allen CD, Macalady AK, Chenchouni H. *et al.* A global overview of drought and heat-induced tree mortality reveals emerging climate change risks for forests. *For Ecol Manage* 2010;**259**:660–84. https://doi.org/10.1016/j.foreco.2009.09.001.

Allen CD, Breshears DD, McDowell NG. On underestimation of global vulnerability to tree mortality and forest die-off from hotter drought in the Anthropocene. *Ecosphere* 2015;**6**:art129–55. https://doi.org/10.1890/ES15-00203.1.

Anderegg WRL, Kane JM, Anderegg LDL. Consequences of widespread tree mortality triggered by drought and temperature stress. *Nat Clim Chang* 2013;**3**:30–6. https://doi.org/10.1038/nclimate1635.

Augspurger CK, Bartlett EA. Differences in leaf phenology between juvenile and adult trees in a temperate deciduous forest. *Tree Physiol* 2003;**23**:517–25. https://doi.org/10.1093/treephys/23.8.517.

Baeten L, Bruelheide H, van der Plas F. *et al.* Identifying the tree species compositions that maximize ecosystem functioning in European forests. *J Appl Ecol* 2019;**56**:733–44. https://doi.org/10.1111/1365-2664.13308.

Bauhus J, Forrester DI, Gardiner B. *et al.* Ecological stability of mixed-species forests. In: Pretzsch H, Forrester DI, Bauhus J. *et al.* (eds) *Mixed-Species Forests*. Berlin, Heidelberg: Springer, 2017a, 337–82. doi: https://doi.org/10.1007/978-3-662-54553-9_7.

Bauhus J, Forrester DI, Pretzsch H. *et al.* Silvicultural options for mixed-species stands. In: Pretzsch H, Forrester DI, Bauhus J. *et al.* (eds) *Mixed-Species Forests*. Berlin, Heidelberg: Springer, 2017b, 433–501. doi: https://doi.org/10.1007/978-3-662-54553-9_9.

Bauhus J, Van Winden AP, Nicotra AB. Aboveground interactions and productivity in mixed-species plantations of *Acacia mearnsii* and *Eucalyptus globulus*. *Can J For Res* 2004;**34**:686–94. https://doi.org/10.1139/x03-243.

Bennett AC, McDowell NG, Allen CD. *et al.* Larger trees suffer most during drought in forests worldwide. *Nat Plants* 2015;**1**:15139. https://doi.org/10.1038/nplants.2015.139.

Bigler C, Bräker OU, Bugmann H. *et al.* Drought as an inciting mortality factor in Scots Pine Stands of the Valais, Switzerland. *Ecosystems* 2006;**9**:330–43. https://doi.org/10.1007/s10021-005-0126-2.

Bigler C, Gavin DG, Gunning C. *et al.* Drought induces lagged tree mortality in a subalpine forest in the Rocky Mountains. *Oikos* 2007;**116**:1983–94. https://doi.org/10.1111/j.2007.0030-1299.16034.x.

Binkley D. Mixtures of nitrogen-fixing and non-nitrogen-fixing tree species. In: Cannell MGR, Malcolm DC, Robertson PA, eds. *The Ecology of Mixed Species Stands of Trees*. London: Blackwell Scientific, 1992; 99–123.

Binkley D, Dunkin KA, DeBell D. *et al.* Production and nutrient cycling in mixed plantations of Eucalyptus and Albizia in Hawaii. *For Sci* 1992;**38**:393–408. https://doi.org/10.1093/forestscience/38.2.393.

CABI. *Alnus glutinosa (European alder)*, CABI Compend. CABI International. 2022. doi: https://doi.org/10.1079/cabicompendium.4574.

Cailleret M, Jansen S, Robert EMR. *et al.* A synthesis of radial growth patterns preceding tree mortality. *Glob Chang Biol* 2017;**23**:1675–90. https://doi.org/10.1111/gcb.13535.

Charbonnier F, Maire GL, Dreyer E. *et al.* Competition for light in heterogeneous canopies: application of MAESTRA to a coffee (*Coffea arabica* L.) agroforestry system. *Agric For Meteorol* 2013;**181**:152–69. https://doi.org/10.1016/j.agrformet.2013.07.010.

Clark JS, Iverson L, Woodall CW. *et al.* The impacts of increasing drought on forest dynamics, structure, and biodiversity in the United States. *Glob Chang Biol* 2016;**22**:2329–52. https://doi.org/10.1111/gcb.13160.

Davis KT, Dobrowski SZ, Holden ZA. *et al.* Microclimatic buffering in forests of the future: the role of local water balance. *Ecography* 2018;**42**:1–11. https://doi.org/10.1111/ecog.03836.

Dee DP, Uppala SM, Simmons AJ. *et al.* The ERA-interim reanalysis: configuration and performance of the data assimilation system. *Q J Roy Meteorol Soc* 2011;**137**:553–97. https://doi.org/10.1002/qj.828.

Dirnberger GF, Sterba H. A comparison of different methods to estimate species proportions by area in mixed stands. *For Syst* 2014;**23**:534–46. https://doi.org/10.5424/fs/2014233-06027.

Dong TL, Forrester DI, Beadle C. *et al.* Effects of light availability on crown structure, biomass production, light absorption and light-use efficiency of *Hopea odorata* planted within gaps in acacia hybrid plantations. *Plant Ecol Divers* 2016;**9**:535–48. https://doi.org/10.1080/17550874.2016.1262471.

Duursma RA, Medlyn BE. MAESPA: a model to study interactions between water limitation, environmental drivers and vegetation function at tree and stand levels, with an example application to [CO2] × drought interactions. *Geosci Model Dev* 2012;**5**:919–40. https://doi.org/10.5194/gmd-5-919-2012.

Feng Y, Schmid B, Loreau M. *et al.* Multispecies forest plantations outyield monocultures across a broad range of conditions. *Science* 2022;**376**:865–8. https://doi.org/10.1126/science.abm6363.

Forrester DI. The spatial and temporal dynamics of species interactions in mixed-species forests: from pattern to process. *For Ecol Manage* 2014;**312**:282–92. https://doi.org/10.1016/j.foreco.2013.10.003.

Forrester DI, Lancaster K, Collopy JJ. *et al.* Photosynthetic capacity of *Eucalyptus globulus* is higher when grown in mixture with *Acacia mearnsii*. *Trees - Struct Funct* 2012;**26**:1203–13. https://doi.org/10.1007/s00468-012-0696-5.

Forrester DI, Collopy JJ, Beadle CL. *et al.* Effect of thinning, pruning and nitrogen fertiliser application on light interception and light-use efficiency in a young *Eucalyptus nitens* plantation. *For Ecol Manage* 2013;**288**:21–30. https://doi.org/10.1016/j.foreco.2011.11.024.

Forrester DI. Growth responses to thinning, pruning and fertiliser application in eucalyptus plantations: a review of their production ecology and interactions. *For Ecol Manage* 2013;**310**:336–47. https://doi.org/10.1016/j.foreco.2013.08.047.

Forrester DI, Ammer C, Annighöfer PJ. *et al.* Effects of crown architecture and stand structure on light absorption in mixed and monospecific *Fagus sylvatica* and *Pinus sylvestris* forests along a productivity and climate gradient through Europe. *J Ecol* 2018;**106**:746–60. https://doi.org/10.1111/1365-2745.12803.

Forrester DI, Ammer C, Annighöfer PJ. *et al.* Predicting the spatial and temporal dynamics of species interactions in *Fagus sylvatica* and *Pinus sylvestris* forests across Europe. *Forest Ecol Manage* 2017a;**405**:112–33. https://doi.org/10.1016/j.foreco.2017.09.029.

Forrester DI, Tachauer IHH, Annighoefer P. *et al.* Generalized biomass and leaf area allometric equations for European tree species incorporating stand structure, tree age and climate. *For Ecol Manage* 2017b;**396**:160–75. https://doi.org/10.1016/j.foreco.2017.04.011.

Forrester DI. Linking forest growth with stand structure: tree size inequality, tree growth or resource partitioning and the asymmetry of competition. *For Ecol Manage* 2019;**447**:139–57. https://doi.org/10.1016/j.foreco.2019.05.053.

Forrester DI, Rodenfels P, Haase J. *et al.* Tree-species interactions increase light absorption and growth in Chinese subtropical mixed-species plantations. *Oecologia* 2019;**191**:421–32. https://doi.org/10.1007/s00442-019-04495-w.

Forrester DI, Albrecht AT. Light absorption and light-use efficiency in mixtures of *Abies alba* and *Picea abies* along a productivity gradient. *For Ecol Manage* 2014;**328**:94–102. https://doi.org/10.1016/j.foreco.2014.05.026.

Forrester DI, Pretzsch H. Tamm review: on the strength of evidence when comparing ecosystem functions of mixtures with monocultures. *For Ecol Manage* 2015;**356**:41–53. https://doi.org/10.1016/j.foreco.2015.08.016.

Friedman JH. *A Variable Span Scatterplot Smoother. Laboratory for Computational Statistics*. Stanford, California: Stanford University Technical, 1984a; Report No.5.

Friedman JH. *User's Guide. Laboratory for Computational Statistics*. Stanford, California: Stanford University Technical. 1984b Report No.1. Available at: https://purl.stanford.edu/pd898dq6156.

Garber SM, Maguire DA. The response of vertical foliage distribution to spacing and species composition in mixed conifer stands in Central Oregon. *For Ecol Manage* 2005;**211**:341–55. https://doi.org/10.1016/j.foreco.2005.02.053.

Grace JC, Jarvis PG, Norman JM. Modelling the interception of solar radiant energy in intensively managed stands. *New Zeal J For Sci* 1987;**17**:193–209.

Gressler E, Jochner S, Capdevielle-Vargas RM. *et al.* Vertical variation in autumn leaf phenology of *Fagus sylvatica* L. in southern Germany. *Agric For Meteorol* 2015;**201**:176–86. https://doi.org/10.1016/j.agrformet.2014.10.013.

Gspaltl M, Bauerle W, Binkley D. *et al.* Leaf area and light use efficiency patterns of Norway spruce under different thinning regimes and age classes. *For Ecol Manage* 2013;**288**:49–59. https://doi.org/10.1016/j.foreco.2011.11.044.

Houston, Durrant T, de Rigo D, Caudullo G. *Alnus glutinosa* in Europe: distribution, habitat, usage and threats. *Eur Atlas For Tree Species* 2016;64–5.

IPCC. The physical science basis. In: Stocker TF. *et al.* (eds) *Contribution of Working Group I to the Fifth Assessment Report of the Intergovern- Mental Panel on Climate Change.* Cambridge University Press: Cambridge and New York, NY, 2013. doi: https://doi.org/10.1017/CBO9781107415324.Summary.

IUSS Working Group WRB. *World Reference Base for Soil Resources 2006.* 2nd edn. Rome: World Soil Resources Reports No 103 FAO, 2006. Available at: ftp://ftp.fao.org/agl/agll/docs/wsrr103e.pdf.

Jactel H, Bauhus J, Boberg J. *et al.* Tree diversity drives forest stand resistance to natural disturbances. *Curr For Rep* 2017;**3**:223–43. https://doi.org/10.1007/s40725-017-0064-1.

Klockow PA, Vogel JG, Edgar CB. *et al.* Lagged mortality among tree species four years after an exceptional drought in East Texas. *Ecosphere* 2018;**9**:e02455. https://doi.org/10.1002/ecs2.2455.

Klos RJ, Wang GG, Bauerle WL. *et al.* Drought impact on forest growth and mortality in the Southeast USA: an analysis using forest health and monitoring data. *Ecol Appl* 2009;**19**:699–708. https://doi.org/10.1890/08-0330.1.

Laclau J-P, Bouillet J-P, Gonçalves JLM. *et al.* Mixed-species plantations of *Acacia mangium* and *Eucalyptus grandis* in Brazil 1. Growth dynamics and aboveground net primary production. *For Ecol Manage* 2008;**255**:3905–17. https://doi.org/10.1016/j.foreco.2007.10.049.

Lindner M, Maroschek M, Netherer S. *et al.* Climate change impacts, adaptive capacity, and vulnerability of European forest ecosystems. *For Ecol Manage* 2010;**259**:698–709. https://doi.org/10.1016/j.foreco.2009.09.023.

Lopez OR, Farris-Lopez K, Montgomery RA. *et al.* Leaf phenology in relation to canopy closure in southern Appalachian trees. *Am J Bot* 2008;**95**:1395–407. https://doi.org/10.3732/ajb.0800104.

le Maire G, Nouvellon Y, Christina M. *et al.* Tree and stand light use efficiencies over a full rotation of single- and mixed-species *Eucalyptus grandis* and *Acacia mangium* plantations. *For Ecol Manage* 2013;**288**:31–42. https://doi.org/10.1016/j.foreco.2012.03.005.

Mäkinen H, Isomäki A. Thinning intensity and growth of Scots pine stands in Finland. *For Ecol Manage* 2004;**201**:311–25. https://doi.org/10.1016/j.foreco.2004.07.016.

de Martonne E. Une Nouvelle Fonction CIimatologique: L'Indice d'Aridité (a new climatological function: the aridity index). *La Météorolgie 2* 1926;**2**:449–58.

Medhurst JL, Beadle CL. Crown structure and leaf area index development in thinned and unthinned *Eucalyptus nitens*

plantations. *Tree Physiol* 2001;**21**:989–99. https://doi.org/10.1093/treephys/21.12-13.989.

Medlyn, B. 2004 A MAESTRO retrospective. In: Mencuccini M. *et al.* (eds) *Forest Land-Atmosphere Interface*. Sydney: CAB International, **2004**, 105–21. doi: https://doi.org/10.1079/9780851996776.0105.

Messier C, Bauhus J, Sousa-silva R. *et al.* For the sake of resilience and multifunctionality, let's diversify planted forests! *Conserv Lett*July 2021 2022;**15**:1–8. https://doi.org/10.1111/conl.12829.

Monserud RA, Marshall JD. Allometric crown relations in three northern Idaho conifer species. *Can J For Res* 1999;**29**:521–35. https://doi.org/10.1139/x99-015.

Piepho H-P. An algorithm for a letter-based representation of all pairwise comparisons. *J Comput Graph Stat* 2004;**13**:456–66.

Pinheiro J, Bates D, DebRoy S, Sarkar D. R Core Team, 2018. nlme: Linear and Nonlinear Mixed Effects Models. R package version 3.1-137. Available at: https://cran.r-project.org/package=nlme.

Plaga BNE, Bauhus J, Pretzsch H. *et al.* No date influence of crown architecture and canopy structure on light absorption, light-use efficiency and growth in mixed and pure Pseudotsuga menziesii and Fagus sylvatica forests. *Eur J For Res [Preprint]* doi: 'in review'.

Powers JS, Vargas G, Brodribb TJ. *et al.* A catastrophic tropical drought kills hydraulically vulnerable tree species. *Glob Chang Biol* 2020;**26**:3122–33. https://doi.org/10.1111/gcb.15037.

R Core Team 2020 *R: A Language and Environment for Statistical Computing*. Vienna: R Foundation for Statistical Computing. Available at: https://www.r-project.org/.

Sapijanskas J, Paquette A, Potvin C. *et al.* Tropical tree diversity enhances light capture through crown plasticity and spatial and temporal niche differences. *Ecology* 2014;**95**:2479–92. https://doi.org/10.1890/13-1366.1.

Seidl R, Thom D, Kautz M. *et al.* Forest disturbances under climate change. *Nat Clim Chang* 2017;**7**:395–402. https://doi.org/10.1038/nclimate3303.

Serrano-León H, Nitschke R, Scherer-Lorenzen M. *et al.* Intra-specific leaf trait variability of *F. sylvatica*, *Q. petraea* and *P. abies* in response to inter-specific competition and implications for forest functioning. *Tree Physiol* 2022;**42**:253–72. https://doi.org/10.1093/treephys/tpab109.

Smith AR, Lukac M, Hood R. *et al.* Elevated CO2 enrichment induces a differential biomass response in a mixed species temperate forest plantation. *New Phytol* 2013;**198**:156–68. https://doi.org/10.1111/nph.12136.

Smith DM, Larson BC, Kelty MJ. *et al.*, eds. *The Practice of Silviculture: Applied Forest Ecology*. 9th edition. New York: Wiley, 1997.

Snowdon P. A ratio estimator for bias correction in logarithmic regressions. *Can J For Res* 1991;**21**:720–4. https://doi.org/10.1139/x91-101.

Stoneman GL, Crombie DS, Whitford K. *et al.* Growth and water relations of *Eucalyptus marginata* (jarrah) stands in response to thinning and fertilization. *Tree Physiol* 1996;**16**:267–74.

Trugman AT, Anderegg LD, Anderegg WR. *et al.* Why is tree drought mortality so hard to predict? *Trends Ecol Evol* 2021;**36**:520–32. https://doi.org/10.1016/j.tree.2021.02.001.

Vitasse Y. Ontogenic changes rather than difference in temperature cause understory trees to leaf out earlier. *New Phytol* 2013;**198**:149–55. https://doi.org/10.1111/nph.12130.

von Arx G, Dobbertin M, Rebetez M. Spatio-temporal effects of forest canopy on understory microclimate in a long-term experiment in Switzerland. *Agric For Meteorol* 2012;**166-167**:144–55. https://doi.org/10.1016/j.agrformet.2012.07.018.

Wang YP, Jarvis PG. Description and validation of an array model - MAESTRO. *Agric For Meteorol* 1990;**51**:257–80. https://doi.org/10.1016/0168-1923(90)90112-J.

Wang YP, Jarvis PG, Benson ML. Two-dimensional needle-area density distribution within the crowns of Pinus radiata. *For Ecol Manage* 1990;**32**:217–37. https://doi.org/10.1016/0378-1127(90)90172-8.

West PW, Osler GHR. Growth response to thinning and its relation to site resources in Eucalyptus regnans. *Can J For Res* 1995;**25**:69–80. https://doi.org/10.1139/x95-009.

Will RE, Narahari NV, Shiver BD. *et al.* Effects of planting density on canopy dynamics and stem growth for intensively managed loblolly pine stands. *For Ecol Manage* 2005;**205**:29–41. https://doi.org/10.1016/j.foreco.2004.10.002.

Williams AC, McCarthy BC. A new index of interspecific competition for replacement and additive designs. *Ecol Res* 2001;**16**:29–40. https://doi.org/10.1046/j.1440-1703.2001.00368.x.

Zellweger F, Frenne PD, Lenoir J. *et al.* Forest microclimate dynamics drive plant responses to warming. *Science* 2020;**368**:772–5. https://doi.org/10.1126/science.aba6880.

Zhang Y, Chen HYH, Reich PB. Forest productivity increases with evenness, species richness and trait variation: a global meta-analysis. *J Ecol* 2012;**100**:742–9. https://doi.org/10.1111/j.1365-2745.2011.01944.x.